
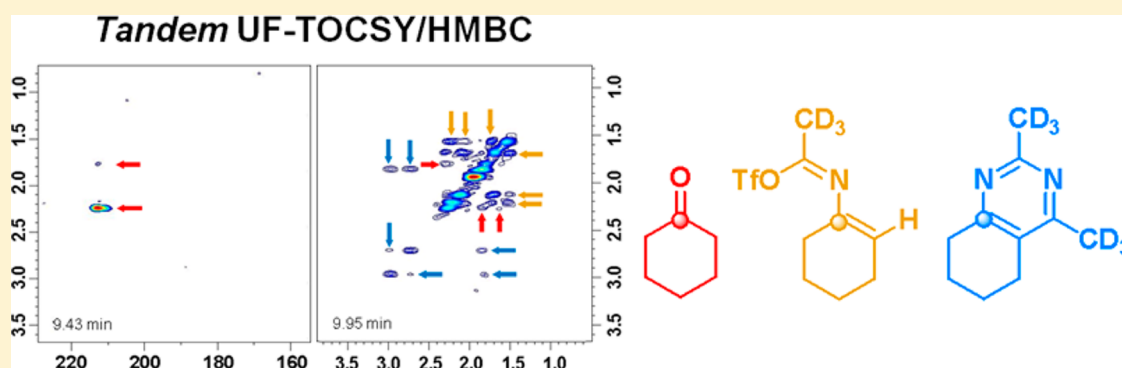


# Discovering Mechanistic Insights by Application of Tandem Ultrafast Multidimensional NMR Techniques

Israel Fernández,<sup>†</sup> María Encarnación Fernández-Valle,<sup>‡</sup> Roberto Martínez-Álvarez,<sup>†</sup> Dolores Molero-Vílchez,<sup>‡</sup> Zulay D. Pardo,<sup>†</sup> Elena Sáez-Barajas,<sup>‡</sup> Ángel Sánchez,<sup>‡</sup> and Antonio Herrera<sup>\*,†,‡</sup>

<sup>†</sup>Departamento de Química Orgánica I and <sup>‡</sup>CAI de RMN y RSE, Facultad de Químicas, Universidad Complutense, 28040 Madrid, Spain

 Supporting Information



**ABSTRACT:** Ultrafast multidimensional NMR acquisition techniques have shown promising capabilities in studies of dynamic systems in real time. The method's characteristics have permitted the focus to be on the mechanistic details of organic reactions. The *tandem* UF-TOCSY/HMBC sequence applied here combines both homonuclear and heteronuclear details and therefore provides complete information about the evolution of a dynamic reaction in real time. The methodology will be applied to find an explanation of the low reactivity of alicyclic ketones such as cyclohexanone in reactions with triflic anhydride and aliphatic nitriles, which leads to bicyclic pyrimidines.

## 1. INTRODUCTION

Multidimensional NMR plays an essential role in current spectroscopy. Traditionally, *n*D NMR experiments are collected as an array of 1D scans<sup>1,2</sup> and therefore need a long time (up to several hours) to complete the acquisition of the data. This is perhaps the main drawback and the most significant barrier to such applications. Today, ultrafast (UF) 2D NMR is a very promising methodology since it involves the most drastic reduction of experiment time because the acquisition of 2D NMR data can be carried out in a single scan.<sup>3,4</sup> As a result of this revolutionary improvement, UF-NMR techniques have been found to have applications in an increasing number of areas related to organic<sup>5,6</sup> and analytical chemistry,<sup>7</sup> as well as biomedical<sup>8</sup> and biological studies.<sup>9</sup> Real-time NMR measurements have provided unique opportunities to discover spectroscopic evidence of mechanistic aspects for known chemical reactions that have remained open for many years. One of these not-yet-well-known-but-important systems is the reaction among carbonyl compounds such as ketones with strong electrophiles such as triflic anhydride (Tf<sub>2</sub>O) and nitriles that leads to pyrimidines and related N-heterocycles.<sup>10</sup> According to this general procedure, different types of heterocycles can be obtained after the nucleophilic trapping

of the cationic species formed from carbonyl compounds and Tf<sub>2</sub>O in the presence of nitriles.

Because of the lack of knowledge about the participant species, we decided to apply UF 2D NMR techniques to monitor systems in real time to obtain mechanistic insights from these reactions. For these reasons, we have studied the synthesis of alkylpyrimidines from aliphatic ketones **1** (R, R' = alkyl) by amplitude-modulated, two-dimensional homonuclear UF-TOCSY.<sup>11</sup> Additionally, a constant-time selective multiwindowed two-dimensional heteronuclear UF-HSQC was also applied to monitoring the reaction with arylalkyl ketones **1** (R = aryl, R' = alkyl), which leads to substituted pyrimidines **5**.<sup>12</sup> Both pulse sequences are shown in Scheme 1.

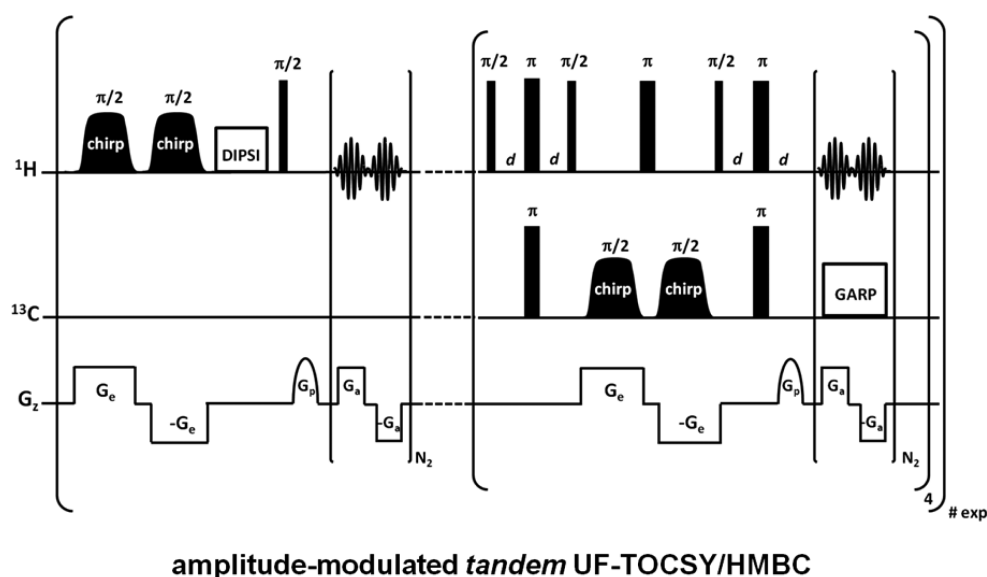
In these studies, spectroscopic data about the presence of intermediates formed by nucleophilic capture by acetonitrile-*d*<sub>3</sub>, such as the ketone-Tf<sub>2</sub>O-acetonitrile complex **2**, and further evolution to aliphatic and olefinic intermediates **3** and **4** (Scheme 2) have been obtained.

Additional decisive mechanistic arguments resulted from monitoring the reaction of acetophenone with Tf<sub>2</sub>O and *d*<sub>3</sub>-acetonitrile by UF-HMBC.<sup>13</sup> The UF sequence used consisted

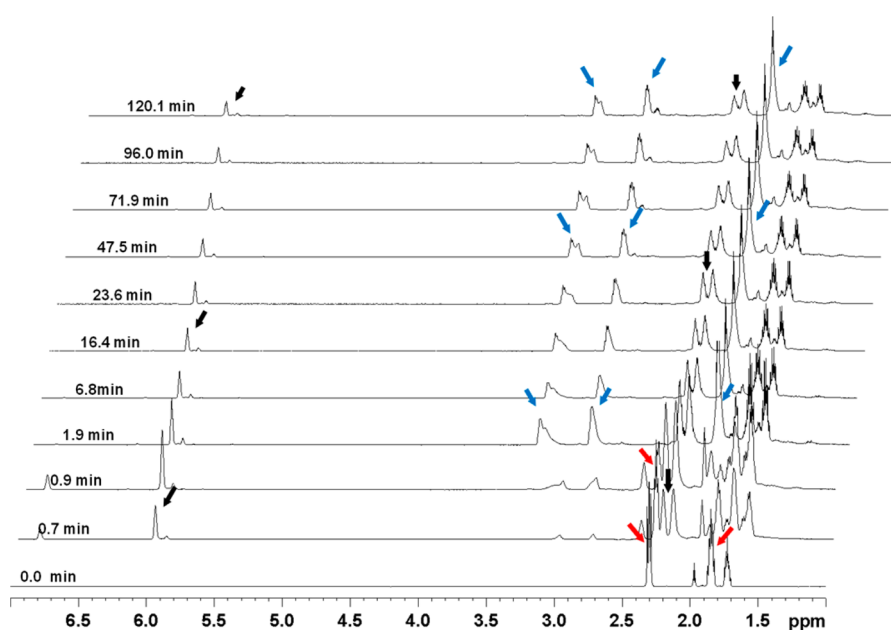
Received: June 9, 2014

Published: August 4, 2014





**Figure 1.** Pulse sequence for the *tandem* UF-TOCSY/HMBC. Both amplitude-modulated UF-TOCSY (1 scan) and UF-HMBC (4 scans) were applied. The UF-HMBC part of the sequence used consists of a HSQC sequence in which the delay,  $d$ , is set to 25 ms in order to monitor  $^2J$  and  $^3J$  H,C couplings.



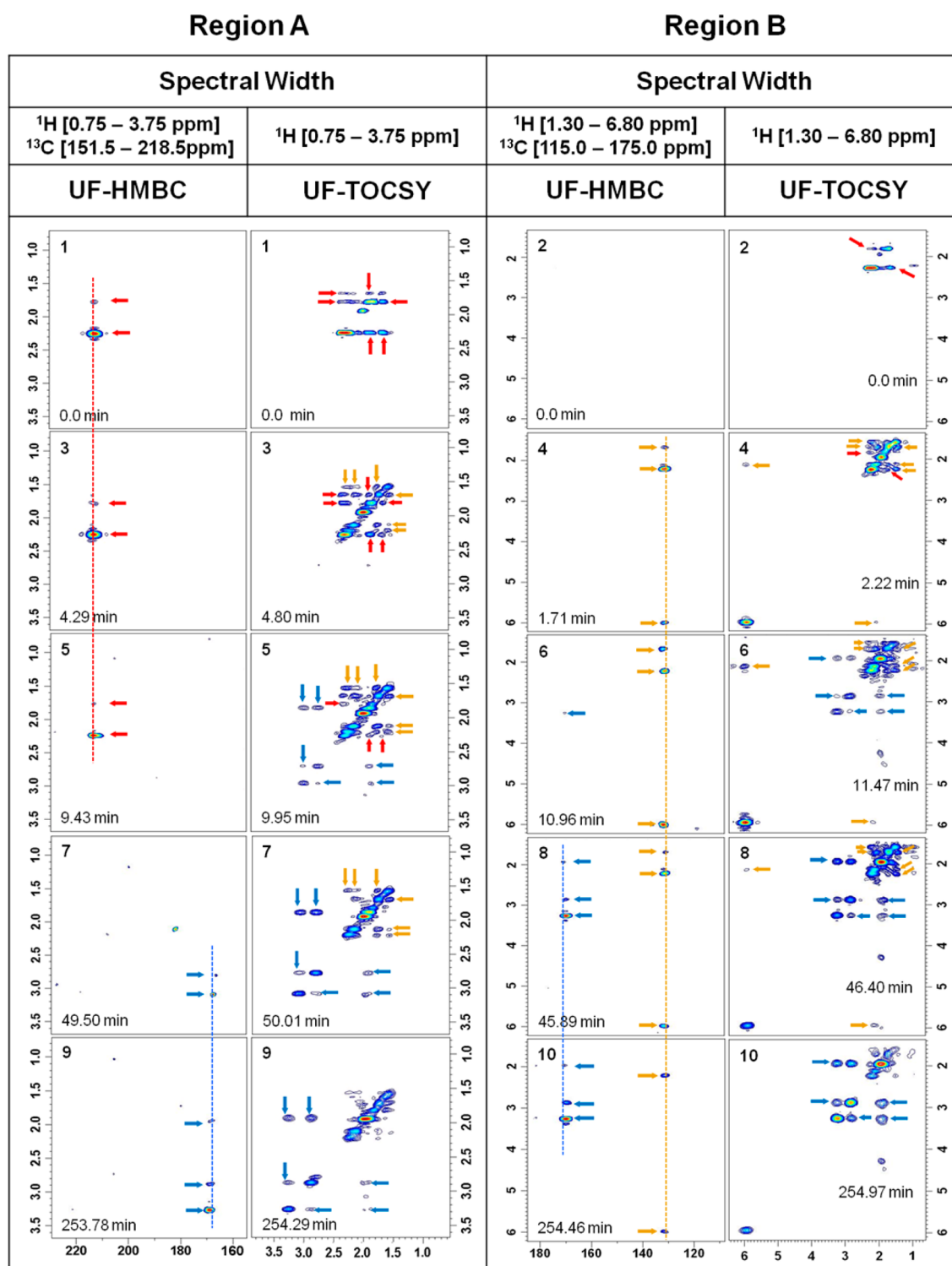
**Figure 2.** Real-time 1D  $^1\text{H}$  NMR spectra recorded as a function of time. Colored arrows show the positions of specific signals from products and intermediates participating in the reaction between  $^{13}\text{C}$ -carbonyl-cyclohexanone (**9**) (300 mM) and triflic anhydride (450 mM) in acetonitrile- $d_3$  (as both a coreactant and solvent) at 278 K. The red arrows indicate the signal of methylene groups from starting cyclohexanone. Blue arrows show signals from ring methylene groups of the final pyrimidine (**10**). Depicted with black arrows are new olefinic and aliphatic signals originated from the beginning of the reaction, whose intensity slowly decreases with the time.

## 2. MATERIALS AND METHODS

To obtain information about how scalar homonuclear TOCSY H,H- and heteronuclear HMBC H,C-correlations evolve in real time, we decided to attempt to monitor the reaction in Scheme 4 from labeled  $^{13}\text{C}$ -carbonyl-cyclohexanone **9**, triflic anhydride, and acetonitrile- $d_3$ . To address information regarding the intermediate species formed, different zones of interest covering the aliphatic and olefinic range were studied.

Two spectral regions A and B were selected for these observations, involving 3.0 and 5.5 ppm along the  $^1\text{H}$  and  $\sim 60$  ppm along the  $^{13}\text{C}$  dimension. Region A covers H,H-

correlations among aliphatic protons and their correlations with carbonyl and aromatic carbons; the second region B shows the H,H-correlations among aliphatic and olefinic protons and their correlations with olefinic carbons (Figure 3). A scheme of these *tandem* pulse sequences is illustrated in Figure 1 and basically consists of a series of amplitude modulated continuous spatial encoding UF-TOCSY and UF-HMBC sequences.<sup>18</sup> These UF 2D NMR data sets were collected on a Bruker 500 MHz NMR spectrometer using a standard BBO z-gradient probe at 278 K.



**Figure 3.** Representative selection of real-time 2D UF-HMBC/TOCSY NMR spectra arising from the reaction of triflic anhydride, labeled  $^{13}\text{C}$ -carbonyl-cyclohexanone (**9**) and acetonitrile- $d_3$ . Two different spectral ranges were studied. Region A: 151.5–218.5 ppm for  $^{13}\text{C}$  and 0.75–3.75 ppm for  $^1\text{H}$ . Region B: 115.0–185.0 ppm for  $^{13}\text{C}$  and 1.30–6.80 ppm for  $^1\text{H}$ . Spectra show HMBC and TOCSY cross-peaks from starting ketone (**9**, red arrows) and final pyrimidine (**10**, blue arrows), as well as new signals that rise and fall (dark yellow arrows).

The experiment started with a solution of 18.6  $\mu\text{L}$  of cyclohexanone in 0.5 mL of acetonitrile, which was pretuned and preshimmed prior to the injection of a small amount (44.8  $\mu\text{L}$ ) of  $\text{Ti}_2\text{O}$ . A mixing device was used for this injection, including a syringe feeding directly into the NMR tube inside the magnet (see the Supporting Information). Data collection was initiated prior to the injection of  $\text{Ti}_2\text{O}$ . In region A, each

UF-TOCSY acquired in one scan was recorded in 0.123 s, and every UF-HMBC (0.148 s/scan), acquired in 4 scans with a delay of 5 s between, was recorded in 20.59 s. The total time per UF-TOCSY/HMBC sequence was 35.75 s, including the repetition time (10 s).

In region B, each UF-TOCSY acquired in one scan was recorded in 0.106 s and every UF-HMBC (0.131 s/scan),

acquired in 4 scans with a delay of 5 s between, was recorded in 20.52 s. The total time per UF-TOCSY/HMBC sequence was 35.66 s, including the repetition time (10 s).

This application of *tandem* UF-TOCSY/HMBC experiment targeting different windows of interest permitted the complete observation of homonuclear and long-range heteronuclear correlations. Both data sets belonging to a single acquisition window were obtained in the same real-time acquisition batch. The resulting time-domain signals were processed into 2D spectra in the usual ultrafast fashion and characterized using custom-written Matlab scripts.

### 3. RESULTS AND DISCUSSION

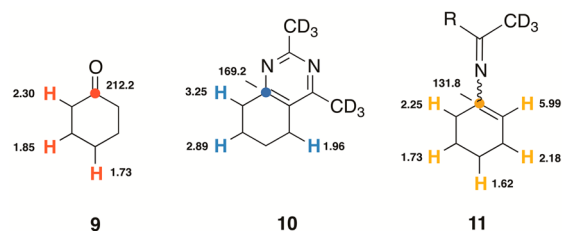
**3.1. One-Dimensional Real-Time Measurements.** First, a series of 1D  $^1\text{H}$  NMR spectra were obtained at increasing times to explore the regions where changes had taken place. Beside the signals from starting ketone (red arrows) and final pyrimidine (blue arrows), the results show (Figure 2) the formation of additional new transient signals in the olefinic and the aliphatic regions. The rise and fall of the intensity over time of some of these new signals indicates their probable character as intermediates.

**3.2. Ultrafast 2D TOCSY/HMBC Correlations.** The structural details of the intermediates cannot be determined from 1D  $^1\text{H}$  NMR experiments. It is necessary to obtain additional information from real-time 2D ultrafast homo- and heteronuclear *tandem* correlation techniques. The UF-TOCSY/HMBC experiment was applied to the reaction studied. According to the temporal series of  $^1\text{H}$  NMR experiments, two different areas were selected for examination by UF-TOCSY/HMBC experiments. The first was focused on the aliphatic region for  $^1\text{H}$  (0.75–3.75 ppm) and the carbonyl-aromatic for  $^{13}\text{C}$  (151.5–218.5 ppm) to monitor the evolution of the starting cyclohexanone (region A). The second region studied was the aliphatic-olefinic area for  $^1\text{H}$  (1.30–6.80 ppm) and the olefinic range for  $^{13}\text{C}$  (115.0–175.0 ppm) (region B). Both regions should show information about the evolution of the different intermediates and products formed.

A total of 500 UF-TOCSY/HMBC spectra were taken in kinetic progression at ca. 10 s delay. Data acquisition was begun immediately prior to the sudden addition of triflic anhydride to a solution of ketone (**9**) in acetonitrile- $d_3$ . Figure 3 illustrates a series of 5 pairs of UF-TOCSY/HMBC experiments for each region studied, which were recorded at increasing times and numbered (odd numbers for region A and even for region B). In these spectra, colored arrows denote cross-peaks that belong to the participant species in the reaction. Vertical colored lines show the evolution with time of the important HMBC correlations from the carbonyl (red), aromatic (blue), and olefinic (dark yellow) C atoms. The number of vertical lines found corresponds to the number of different HMBC correlations, where the carbonyl C atom participates or, in other words, to the number of species present and detected in the reaction. Values of chemical shifts of H and C nuclei from starting cyclohexanone **9** and final pyrimidine **10** are shown in Scheme 5.

UF-HMBC spectra 1, 3, and 5 from region A in Figure 3 show heteronuclear cross-peaks from starting product cyclohexanone **9** ( $^{13}\text{C}$  at 212.2 ppm with  $^1\text{H}$  at 1.85 and 2.30 ppm; red arrows), which are absent after 9.43 min. HMBC cross-peaks from final pyrimidine **10** ( $^{13}\text{C}$  at 169.2 ppm with  $^1\text{H}$  at 1.96, 2.89, and 3.25 ppm; blue arrows) are present in the final UF-HMBC 9, although they rise in UF-HMBC 7. Homo-

Scheme 5



nuclear UF-TOCSY experiments 1, 3, and 5 in region A show aliphatic correlations from ketone **9** (red arrows) observed at 2.30/1.85, 2.30/1.73, and 1.85/1.73 ppm. Pyrimidine **10** presents TOCSY correlations from 9.95 min (UF-TOCSY 5, blue arrows) at 3.25/2.89, 3.25/1.96, and 2.89/1.96 ppm. Moreover, from the first moments of the reaction at 4.80 min, in UF-TOCSY spectra 3–7, it is possible to observe additional cross-peaks (dark yellow arrows), which rise at 2.25/1.62, 2.18/1.62, and 1.73/1.62. These signals, whose intensity rise and fall with the time, apparently belong to a new structure with the character of an intermediate.

UF-HMBC spectra from region B in Figure 3 bring crucial information about the structure of the intermediate detected by UF-TOCSY spectra in region A. Beside the above-mentioned UF-HMBC cross-peaks from pyrimidine (blue arrows) shown in spectra UF-HMBC 6, 8, and 10, a new group of UF-HMBC cross-peaks, from an olefinic carbon with aliphatic and olefinic protons, can be observed from UF-HMBC spectra 4 ( $^{13}\text{C}$  at 131.8 ppm with  $^1\text{H}$  at 1.73, 2.25, and 5.99 ppm, dark yellow arrows). This group of signals is present from the beginning (1.71 min) until the last moments of the reaction (254.46 min). Their intensity first rises and thereafter decreases slowly with the time, showing the character of a stable intermediate. According to the data observed in UF-HMBC spectra, it follows that an olefinic moiety must be present in the reaction core of the intermediate candidate. To explain the nature of the cross-peaks observed, we propose an iminic-type intermediate **11** (Scheme 5), formed from cyclohexanone **9** under nucleophilic trapping and further elimination of triflic acid.

**3.3. Modeling.** To aid in the structural elucidation of the actual reaction intermediate **11**, the observed experimental  $^1\text{H}$  and  $^{13}\text{C}$  NMR chemical shifts were compared to those estimated using Advanced Chemistry Development, Inc. (ACD/Laboratories) Software V8.0. Similarly, more accurate estimation of the  $^{13}\text{C}$  NMR shifts were carried out using Density Functional Theory (DFT) calculations within the Gauge-Independent Atomic Orbital (GIAO) approximation (see the Supporting Information).

Table 1 contains observed and calculated data from starting  $^{13}\text{C}$ -carbonyl-cyclohexanone **9** and final 2,4-dimethyl-5,6,7,8-tetrahydroquinazoline- $d_6$  **10**, as well as from the side product cyclohexenyl-triflate **15** and the potential reactive intermediates **13** and **14**. As readily seen in Table 1, data obtained at the GIAO-PCM(acetonitrile)-B3LYP/6-31+G\* level seem to correlate better with the experimental chemical shifts than those values obtained at the GIAO-PCM(acetonitrile)-M06-2X/6-31+G\* level, which slightly overestimate the corresponding  $^{13}\text{C}$  NMR chemical shifts within ca. 10 ppm. Despite that, three possible structures for the unknown olefinic intermediate **11** can be envisaged: (a) species **12** where the iminic carbon atom bears a OTf substituent (the corresponding *s-cis* isomer is 1.9 kcal/mol less stable than the *s-trans-12*), (b) species **13**, the



Table 1. Observed and Calculated Chemical Shifts of the Different Species Involved in the Reaction

		Observed (CD <sub>3</sub> CN) <sup>a</sup>		Calculated (CDCl <sub>3</sub> ) <sup>b</sup>	Calculated GAUSSIAN 09 <sup>d</sup>	
		<sup>1</sup> H	<sup>13</sup> C	<sup>1</sup> H y <sup>13</sup> C	<sup>13</sup> C B3LYP	<sup>13</sup> C M062X
9		H <sub>2</sub> : 2.30 H <sub>3</sub> : 1.85 H <sub>4</sub> : 1.73	C1: 212.2	H <sub>2</sub> : 2.2 H <sub>3</sub> : 1.6 H <sub>4</sub> : 1.4 C <sub>1</sub> : 211.5	C <sub>1</sub> : 211.6	
10		H <sub>3</sub> : 1.96 H <sub>5</sub> : 2.89 H <sub>6</sub> : 3.25	C <sub>1</sub> : 169.2	H <sub>3</sub> : 2.3 H <sub>4</sub> : 1.9 H <sub>5</sub> : 1.9 H <sub>6</sub> : 2.9 C <sub>1</sub> : 163.1 C <sub>2</sub> : 126.0	C <sub>1</sub> : 161.7 C <sub>2</sub> : 124.3	C <sub>1</sub> : 181.7 C <sub>2</sub> : 140.3
12				H <sub>2</sub> : 5.8 H <sub>3</sub> : 2.2 H <sub>4</sub> : 1.5 H <sub>5</sub> : 1.8 H <sub>6</sub> : 2.0 C <sub>1</sub> : 140.7 C <sub>2</sub> : 113.7	C <sub>1</sub> : 137.3 C <sub>2</sub> : 130.0	C <sub>1</sub> : 158.1 C <sub>2</sub> : 128.5
13		5.99 2.25 2.18 1.73 1.62	C <sub>1</sub> : 131.8 C <sub>2</sub> : 124.9 <sup>e</sup>	H <sub>2</sub> : 4.7 H <sub>3</sub> : 2.2 H <sub>4</sub> : 1.7 H <sub>5</sub> : 1.7 H <sub>6</sub> : 2.8 C <sub>1</sub> : 136.7 C <sub>2</sub> : 123.4	C <sub>1</sub> : 118.9 C <sub>2</sub> : 146.4	C <sub>1</sub> : 135.0 C <sub>2</sub> : 160.7
14				H <sub>2</sub> : 5.5 H <sub>3</sub> : 2.1 H <sub>4</sub> : 1.4 H <sub>5</sub> : 1.7 H <sub>6</sub> : 2.1 C <sub>1</sub> : 160.4 C <sub>2</sub> : 113.1	C <sub>1</sub> : 144.1 C <sub>2</sub> : 116.4	C <sub>1</sub> : 160.2 C <sub>2</sub> : 125.6
15		H <sub>2</sub> : 5.83	C <sub>1</sub> : 150.3	H <sub>2</sub> : 5.9 H <sub>3</sub> : 2.2 H <sub>4</sub> : 1.6 H <sub>5</sub> : 1.6 H <sub>6</sub> : 2.7 C <sub>1</sub> : 153.2 C <sub>2</sub> : 117.5	C <sub>1</sub> : 146.7 C <sub>2</sub> : 124.0	C <sub>1</sub> : 157.4 C <sub>2</sub> : 137.5

<sup>a</sup>See the Supporting Information <sup>b</sup>Averaged values of chemical shifts, ACD/Laboratories (Release 8.00). <sup>c</sup>Differences between observed and calculated chemical shifts are due to the nature of solvent. <sup>d</sup>Calculated with respect to TMS (<sup>13</sup>C = TMS value Gaussian09 – value <sup>13</sup>C compound Gaussian09). <sup>e</sup>Obtained from traditional 2D HSQC spectra.

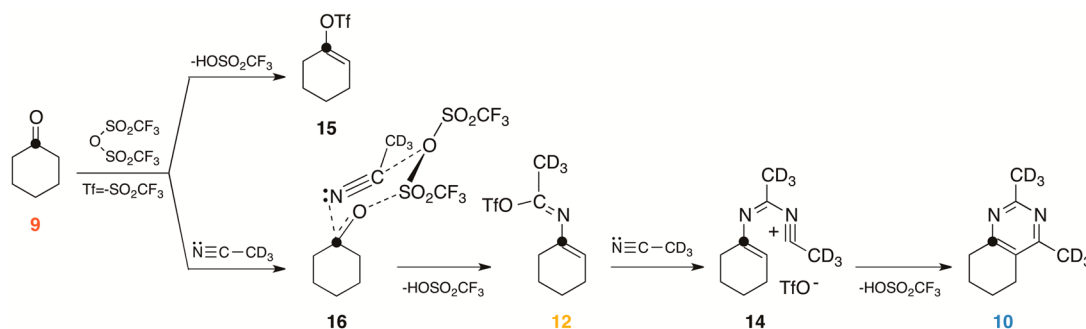


Figure 4. Proposed mechanism for the reaction of cyclohexanone (9), triflic anhydride, and acetonitrile-*d*<sub>3</sub> in accordance with the structural insight gained from the ultrafast NMR experiments and modeling studies.

ionic-pair counterpart of **12** formed upon release of the TfO<sup>-</sup> moiety, and (c) species **14** formed from **12** or **13** upon addition of a new molecule of nitrile. From the data in Table 1, it can be suggested that the structure of **11** corresponds to species **12**, in view of the good correlation between the observed and computed <sup>13</sup>C NMR chemical shifts of the olefinic carbon atoms (deviation of only ca. 5 ppm).

With the above data in hand, the following sequence of events in the reaction of cyclohexanone and triflic anhydride in the presence of acetonitrile can be proposed (Figure 4). First, nucleophilic attack from the lone-pair of the oxygen atom of carbonyl group of **9** to Tf<sub>2</sub>O occurs. This enhances the electrophilicity of the carbonyl carbon atom allowing the nucleophilic addition of the nitrile and leading to a short-lived intermediate **16**. This type of intermediate has already been detected by UF-HMBC and HSQC.<sup>12,13</sup> A small amount of vinyl triflate **15** is usually observed, although in this case it must be below the detection limit. Subsequent elimination of the TfOH from **16** leads to a new and unexpected iminic intermediate species **12** (detected in the ultrafast experiment). The formation of this relatively stable covalent intermediate explains the lack of reactivity of alicyclic ketones in comparison with aliphatic and aliphatic-aromatic ketones. In the case of nonsymmetric alicyclic ketones, similarly to the case of aliphatic ketones, the regioselectivity of the imine intermediates **12** formed would be determined by the different possible eliminations of TfOH from intermediate **16**. The slow solvolytic evolution of **12**, which takes place upon addition of a new molecule of nitrile, forms the nitrilium salt-intermediate **14**. A final 6π-electrocyclization reaction affords the pyrimidinic reaction product **10**, releasing a new molecule of TfOH. Other possible nitrilium salt-intermediates have been detected previously,<sup>12</sup> but in this case, there is not enough time to detect them due to their low stability.

#### 4. CONCLUSIONS

Ultrafast NMR methodology has proven to be an excellent procedure to be applied to studies with organic reactions. Using this combined UF-TOCSY/HMBC sequence, it was possible to gain new mechanistic insights in the reaction of ketones with nitriles in the presence of triflic anhydride. Starting from labeled <sup>13</sup>C-carbonyl-labeled cyclohexanone, it was possible to detect for the first time the presence of a new iminic intermediate (**12**), which explains the lack of reactivity of alicyclic ketones in the formation of pyrimidines promoted by triflic anhydride and alkyl nitriles. Its structure could be established by combining data obtained from the tandem UF-TOCSY/HMBC sequence, with estimations of NMR chemical shifts by modeling. Both data sets are in very good agreement with the proposed structures for the participating species. In summary, we believe once again that the real-time dynamic combined homonuclear/heteronuclear ultrafast methodology described in this work is a powerful NMR tool that permits the acquisition of spectroscopic details in standard conditions for mechanistic studies of dynamic systems.

#### 5. EXPERIMENTAL SECTION

**General Methods.** All starting materials were purchased from commercial suppliers and used without purification. NMR spectra were recorded at 500 MHz. The <sup>1</sup>H and <sup>13</sup>C chemical shifts are reported in parts per million (δ) referenced to residual solvent signals at δ<sub>H/C</sub> 1.94/118.3 (acetonitrile-*d*<sub>3</sub>) relative to tetramethylsilane (TMS) as internal standard.

**Monitoring the Reaction of <sup>13</sup>C-Carbonyl-cyclohexanone (**9**) with Triflic Anhydride (Tf<sub>2</sub>O) and Acetonitrile-*d*<sub>3</sub>. Formation of 2,4-Dimethyl-5,6,7,8-tetrahydroquinazoline-*d*<sub>6</sub> (**10**).** A solution of 18.6 μL (300 mM) of <sup>13</sup>C-carbonyl-cyclohexanone in 0.5 mL of acetonitrile-*d*<sub>3</sub> was prepared and added to a 5 mm NMR tube, which was located inside of the magnet. From outside the spectrometer, 44.8 μL (450 mM) of trifluoromethanesulfonic anhydride (Tf<sub>2</sub>O) was injected into the NMR tube using a fast mixing device, consisting of a long Teflon tube that connected a syringe with a Luer-lock tip to the reaction mixture (see the Supporting Information). The NMR tube was fitted with a cap with a hole and a bearing to minimize oscillations of the injection tube. In the fully loaded position, the injection tube contained, in order from the bottom tip upward: an air bubble of ca. 50 μL, the reactant to be injected (Tf<sub>2</sub>O), and another air bubble (about 100 μL). The upper part of the injection tube was filled with organic solvent (acetonitrile-*d*<sub>3</sub>) to efficiently propagate the pressure throughout the mixing device. The bottom end of the injection tube was 1–2 mm inside the solution and well above of the detection coil zone. The vertical position of the NMR tube was adjusted with the tube spinner. Standard NMR adjustments were carried out before starting the experiment.

Acquisition parameters: amplitude modulated, continuous spatial encoding UF-TOCSY/HMBC spectra were collected on a medium field 500 MHz NMR spectrometer at 278 K. Acquisitions were started before the injection of the Tf<sub>2</sub>O. A total of 500 UF-TOCSY/HMBC were recorded for each spectral region studied.

Region A encompassed 0.75–3.75 ppm for <sup>1</sup>H and 151.5–218.5 ppm for <sup>13</sup>C. The acquisition parameters for the UF-TOCSY part of the sequence were bandwidth chirp pulse = 60 kHz; encoding gradient strength  $G_e = 8.03 \text{ G cm}^{-1}$ ; encoding time  $t_1^{\text{max}} = 10 \text{ ms}$ ; acquisition gradient strength  $G_a = 13.91 \text{ G cm}^{-1}$ ; acquisition time  $T_a = 0.294 \mu\text{s}$ ; number of acquisition steps  $N_2 = 64$  cycles of  $\pm$  gradient pairs; gradient switching time = 40 μs. These parameters correspond to a spectral window of  $\text{SW}_1 = 3.2 \text{ ppm}$  and  $\text{SW}_2 = 3.0 \text{ ppm}$ . A sinusoidal purge gradient of  $16.05 \text{ G cm}^{-1}$  during 200 μs was applied before acquisition. Time used for DIPSI sequence was 60 ms, and number of scans  $NS = 1$ . The acquisition parameters for UF-HMBC part of sequence were bandwidth chirp pulse = 50 kHz; encoding gradient strength  $G_e = 26.75 \text{ G cm}^{-1}$ ; encoding time  $t_1^{\text{max}} = 2.5 \text{ ms}$ ; acquisition gradient strength  $G_a = 19.26 \text{ G cm}^{-1}$ ; acquisition time  $T_a = 0.294 \mu\text{s}$ ; number of acquisition steps  $N_2 = 64$  cycles of  $\pm$  gradient pairs; gradient switching time = 40 μs. These parameters correspond to a spectral window of  $\text{SW}_1 = 67.6 \text{ ppm}$  and  $\text{SW}_2 = 3.0 \text{ ppm}$ . A sinusoidal purge gradient of  $16.05 \text{ G cm}^{-1}$  during 200 μs was applied before acquisition. Time used for INEPT block was 25 ms, and number of scans  $NS = 4$  every 5 s.

Region B encompasses 1.30–6.80 ppm for <sup>1</sup>H and 115.0–175.0 ppm for <sup>13</sup>C. The acquisition parameters for UF-TOCSY part of sequence were bandwidth chirp pulse = 60 kHz; encoding gradient strength  $G_e = 8.03 \text{ G cm}^{-1}$ ; encoding time  $t_1^{\text{max}} = 10 \text{ ms}$ ; acquisition gradient strength  $G_a = 40.13 \text{ G cm}^{-1}$ ; acquisition time  $T_a = 0.160 \mu\text{s}$ ; number of acquisition steps  $N_2 = 64$  cycles of  $\pm$  gradient pairs; gradient switching time = 40 μs. These parameters correspond to a spectral window of  $\text{SW}_1 = 5.0 \text{ ppm}$  and  $\text{SW}_2 = 5.2 \text{ ppm}$ . A sinusoidal purge gradient of  $16.05 \text{ G cm}^{-1}$  during 200 μs was applied before acquisition. Time used for DIPSI sequence was 60 ms; number of scans  $NS = 1$ . The acquisition parameters for UF-HMBC part of sequence were bandwidth chirp pulse = 50 kHz; encoding gradient strength  $G_e = 26.75 \text{ G cm}^{-1}$ ; encoding time  $t_1^{\text{max}} = 2.5 \text{ ms}$ ; acquisition gradient strength  $G_a = 32.10 \text{ G cm}^{-1}$ ; acquisition time  $T_a = 0.160 \mu\text{s}$ ; number of acquisition steps  $N_2 = 64$  cycles of  $\pm$  gradient pairs; gradient switching time = 40 μs. These parameters correspond to a spectral window of  $\text{SW}_1 = 60.0 \text{ ppm}$  and  $\text{SW}_2 = 5.0 \text{ ppm}$ . A sinusoidal purge gradient of  $16.05 \text{ G cm}^{-1}$  during 200 μs was applied before acquisition. Time used for INEPT block was 25 ms, and number of scans  $NS = 4$  every 5 s. A suitable processing (shearing, zero filling before the T2 Fourier transformation and filtering) was carried out for all experiments. Spectra were represented in magnitude mode. Such operations were performed using home written routine in MatLab 7.3.0 (Math Works Inc.). For <sup>1</sup>H NMR, <sup>13</sup>C NMR, TOCSY, and

HMBC spectra from starting (9) and final products (15) and (10), registered in standard conditions, see the Supporting Information. Small differences were found in the position of signals from 10 in standard NMR compared with UF-NMR conditions.

**2,4-Dimethyl-5,6,7,8-tetrahydroquinazoline-*d*<sub>6</sub> (10).** <sup>1</sup>H NMR (CD<sub>3</sub>CN): δ 1.81 (m, 4H), 2.60 (m, 2H), 2.71 (m, 2H) ppm. <sup>13</sup>C NMR (125 MHz, CD<sub>3</sub>CN): δ 20.7 (CD<sub>3</sub>-C4), 21.7, 21.9 (C6, C7), 24.0 (C5), 29.0 (CD<sub>3</sub>-C2), 31.7 (C8), 124.4 (C10), 163.0 (C4), 164.0 (C9), 164.5 (C2) ppm. (HRMS-ESI) [M + H]<sup>+</sup> 169.16043; calcd for C<sub>10</sub>H<sub>8</sub>D<sub>6</sub>N<sub>2</sub> 169.16064.

## ■ ASSOCIATED CONTENT

### ■ Supporting Information

Further details regarding experimental procedures, 1D and 2D spectra of products, and Cartesian coordinates and total energies of all species discussed in the text. This material is available free of charge via the Internet at <http://pubs.acs.org>.

## ■ AUTHOR INFORMATION

### Corresponding Author

\*E-mail: [aherrera@quim.ucm.es](mailto:aherrera@quim.ucm.es).

### Notes

The authors declare no competing financial interest.

## ■ ACKNOWLEDGMENTS

The authors acknowledge financial support from MINECO (Grants CTQ2010-14936 and CTQ2013-44303-P). Z.D.P. acknowledges Universidad Complutense de Madrid for a FPI predoctoral fellowship.

## ■ REFERENCES

- (1) Jeener, J. Lecture presented at Ampere International Summer School, Basko Polje, Yugoslavia, 1971.
- (2) Aue, W. P.; Bartholdi, E.; Ernst, R. R. *J. Chem. Phys.* **1976**, *64*, 2229–2246.
- (3) Tal, A.; Frydman, L. *Prog. Nucl. Magn. Reson. Spectrosc.* **2010**, *57*, 241–292.
- (4) Mishkovsky, M.; Frydman, L. *Annu. Rev. Phys. Chem.* **2009**, *60*, 429–448.
- (5) Giraudeau, P.; Lemeunier, P.; Coutand, M.; Doux, J.-M.; Gilbert, A.; Remaud, G. S.; Akoka, S. *J. Spectrosc. Dyn.* **2011**, *1*, 2.
- (6) Queiroz Júnior, L. H. K.; Giraudeau, P.; dos Santos, F. A. B.; de Oliveira, K. T.; Ferreira, A. G. *Magn. Reson. Chem.* **2012**, *50* (7), 496–501.
- (7) (a) Queiroz Júnior, L. H. K.; Queiroz, D. P. K.; Dhooghe, L.; Ferreira, A. G.; Giraudeau, P. *Analyst* **2012**, *137*, 2357–2361. (b) Boisseau, R.; Charrier, B.; Massou, S.; Portais, J. C.; Akoka, S.; Giraudeau, P. *Anal. Chem.* **2013**, *85*, 9751–9757.
- (8) Martineau, E.; Tea, I.; Akoka, S.; Giraudeau, P. *NMR Biomed.* **2012**, *25*, 985–992.
- (9) Le Guennec, A.; Tea, I.; Antheaume, I.; Martineau, E.; Charrier, B.; Pathan, M.; Akoka, S.; Giraudeau, P. *Anal. Chem.* **2012**, *84*, 10831–10837.
- (10) (a) García Martínez, A.; Herrera Fernández, A.; Moreno Jiménez, F.; García Fraile, A.; Subramanian, L. R.; Hanack, M. *J. Org. Chem.* **1992**, *57*, 1627–1630. (b) Herrera, A.; Martínez-Álvarez, R.; Ramiro, P.; Molero, D.; Almy, J. *J. Org. Chem.* **2006**, *71*, 3026–3032. (c) Herrera, A.; Martínez-Álvarez, R.; Chioua, M.; Chioua, R.; Sánchez, A. *Tetrahedron* **2002**, *58*, 10053–10058. (d) Baraznenok, I. L.; Nenajdenko, V. G.; Balenkova, E. S. *Tetrahedron* **2000**, *56*, 3077–3119.
- (11) Herrera, A.; Fernández-Valle, E.; Martínez-Álvarez, R.; Molero, D.; Pardo, Z. D.; Sáez, E.; Gal, M. *Angew. Chem., Int. Ed.* **2009**, *48*, 6274–6277.

(12) Pardo, Z. D.; Olsen, G. L.; Fernández-Valle, M. E.; Frydman, L.; Martínez-Álvarez, R.; Herrera, A. *J. Am. Chem. Soc.* **2012**, *134*, 2706–2715.

(13) Herrera, A.; Fernández-Valle, M. E.; Gutiérrez, E. M.; Martínez-Álvarez, R.; Molero, D.; Pardo, Z. D.; Sáez, E. *Org. Lett.* **2010**, *12* (1), 144–147.

(14) Shrot, Y.; Shapira, B.; Frydman, L. *J. Magn. Reson.* **2004**, *171*, 162–169.

(15) Herrera, A.; Martínez-Álvarez, R.; Ramiro, P.; Chioua, M.; Torres, R. *Tetrahedron* **2002**, *58*, 3755–3764.

(16) Saurí, J.; Espinosa, J. F.; Parella, T. *Angew. Chem., Int. Ed.* **2012**, *51*, 3919–3922. See also: Saurí, J.; Parella, T. *Magn. Reson. Chem.* **2012**, *50*, 717–721.

(17) Donovan, K. J.; Kupče, E.; Frydman, L. *Angew. Chem., Int. Ed.* **2013**, *52*, 4152–4155.

(18) Shrot, Y.; Frydman, L. *J. Chem. Phys.* **2008**, *128* (5), 052209/1–052209/14.